Experimental characteristics of a linear peristaltic actuator

João Falcão Carneiro * and Fernando Gomes de Almeida **

INEGI, Faculdade de Engenharia, Universidade do Porto, Rua Dr. Roberto Frias, s/n, 4200-465 Porto, Portugal
E-Mail: jpbrfc@fe.up.pt, fga@fe.up.pt

Pneumatic systems are widespread whenever linear motion between two endpoints is required. However, mainly due to friction forces, motion control is difficult. This paper explores a different solution, based on a linear peristaltic principle, to overcome this problem. The pneumatic actuator proposed has several potential advantages over conventional ones: long strokes require little added cost, curved motion profiles are possible and friction force at low velocities presents better characteristics than the ones of conventional actuators. This paper presents a preliminary study of elementary experimental characteristics of the proposed solution. It is shown that no stick slip occurs at low velocities, whilst maintaining force capabilities similar to those of conventional actuators.

Keywords: Servopneumatic systems, pneumatic actuators, conventional motion control
Target audience: Pneumatic systems, Servopneumatic systems, Motion control

1 Introduction

Pneumatic systems are widely used in industry for conventional motion between two end points. Pneumatic systems require a low acquisition cost and are typically low maintenance devices. They present, however, some disadvantages, namely they are low efficiency devices and they are hard to accurately control due to the nonlinear nature of friction forces in the actuator seals. Moreover, pneumatic energy has low density, making it hard to use in mobile applications. These features, along with the advent of low cost electronics and electrical motors in recent years, has been increasingly threatening pneumatic solutions in favour of electrical ones. Several studies can be found in literature comparing electrical to pneumatic solutions. For instance, in /1/ and /2/, electrical solutions are concluded to be the best option, even when the application requires constant forces. Literature studies, however, are not consensual. For instance, in /3/ it is shown that despite their lower energy efficiency, when higher velocities are required, pneumatic solutions outperform electrical ones if they are sized using an exergy based criteria instead of a load based criteria.

One important feature that has been preventing a wider use of pneumatic solutions lies in its low control flexibility: if, on the one hand, two end stop motion tasks are very easy to implement, one the other hand it is hard to obtain accurate motion control whenever more complex trajectories are required. In this particular aspect, electrical drives are clearly superior. It would be therefore very interesting to develop pneumatic solutions enabling high accuracy motion control. Several efforts have been made in literature towards that end /4/, /5/, /6/, /7/, /8/, /9/ and it has been shown that accurate motion control is possible with evolved nonlinear control laws, either in trajectory following /6/ or in pick and place tasks /7/. In /6/ tracking errors lower of only a few millimetres were obtained, whilst in /7/ and /4/ control errors up to the encoder resolution (5 and 1 µm, respectively) were achieved, even in the presence of high load changes and without any controller retuning. These control laws, however, are complex and typically require detailed models of the system, namely friction models, making them hard to implement in a massive way.

Given the above scenario, it would be interesting to develop a pneumatic actuator with better friction proprieties, while retaining the features recognized in conventional pneumatics, namely its simplicity and compactness. This interest is further emphasized by the current trend towards the development of human friendly machine interactions, for which the natural compliance of pneumatic systems is of particular interest. Moreover, recent findings have shown that it is possible to generate compressed air using reversible chemical reactions /10/ and to successfully use it for pneumatic actuators /11/, which may open a wide window of opportunities for pneumatic based solutions, namely in mobile applications.

Although very important developments can be found in recent years for some pneumatic components like valves, for instance, technical and scientific research in the development of new pneumatic actuators is scarce. In fact, besides the use of pneumatic muscles (see for example /12/), the only exception to this panorama known by the authors lies in the use of hybrid actuators, where electrical and pneumatic actuators are combined so that the advantages of each of them are used /13/, /14/. This solution, however, is expensive and potentially bulky.

This paper explores the use of a different pneumatic actuation solution, based on a linear peristaltic principle, to overcome this problem. Although this solution has been patented in Germany in the 80's /15/, there isn't, to the best of the authors' knowledge, any published study exploring its proprieties. The solution envisaged is potentially a low cost and compact solution since it only requires a hose and two rollers. It also presents several functional advantages. For instance, the actuation of systems requiring curved trajectories can be easily obtained, contrary to what happens when using conventional actuators. In fact, it is expected that the working principle used in this work can be used with a curved mechanical guide with negligible changes in the system fundamental behaviour. A linear peristaltic actuator can also potentially present beneficial friction proprieties as shown by the absence of stick-slip behaviour at low velocities. Moreover, contrary to what happens when using conventional pneumatic actuators, the use of a flexible hose in a peristaltic actuator greatly reduces the need for accurate alignment between the actuator and the mechanical guide. This means that the overall system price may become potentially lower than the one obtained with conventional actuators. A further advantage of a linear peristaltic actuator lies in the fact that longer strokes are obtained with very little added cost.

This paper presents preliminary experimental results characterizing a prototype of such a solution, a pneumatic linear peristaltic actuator (PLPA). The paper is organized as follows: next section presents the PLPA, namely its working principle, the experimental prototype developed and the mechanical model. Section 3 presents several experimental characteristics of the prototype and finally in section 4 the main conclusions are drawn.

2 Pneumatic linear peristaltic actuator

2.1 Working principle

The linear peristaltic actuator explored in this this work is depicted on Figure 1. The actuator comprises two rollers and a compressed air pressurized hose. When the pressure applied to the chambers creates a pressure difference between them, the resulting force (F_p) acts on the rollers. This force may be divided into two components (cf. Figure 2): a vertical component F_{p_v}, which is absorbed by the roller supports, and a longitudinal component F_{p_l} which, by pushing the rollers, makes them roll. The rollers are connected to a mechanical guide which absorbs forces and torques acting on the system.

One of the main potential advantages of this solution lies in the absence of sliding surfaces along the motion direction. In fact, given the above description, there is virtually no sliding friction between the hose and the roller in the direction of motion. Only rolling resistance exists in this direction. Friction between hose and roller in the direction of motion is actually beneficial as it promotes contact between the hose outer surface and the rollers, allowing rolling to occur. Consequently, friction effects are mainly determined by the ball bearings friction on the rollers (F_{fr_l}), a rolling resistance force. Undesired characteristics like high Coulomb friction or Stribeck effect are therefore expected to be reduced. It should be underlined that sliding friction occurs in the transversal direction (F_{fr_t}), as also shown in Figure 2. This force is undesirable because it is a dissipative force causing loss of energy. However, its effects on motion are expected to be negligible since its direction is mostly orthogonal to the direction of motion.

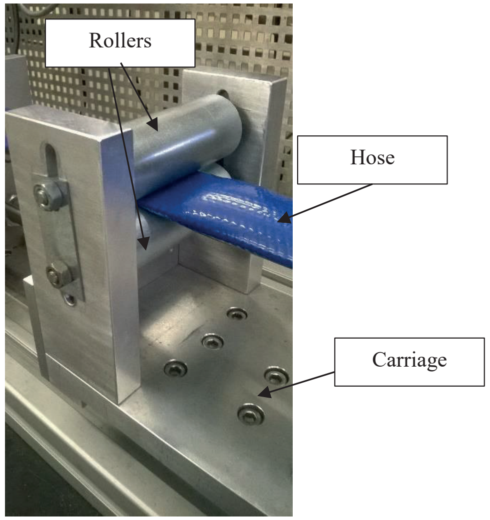

Figure 1: Pneumatic linear peristaltic actuator

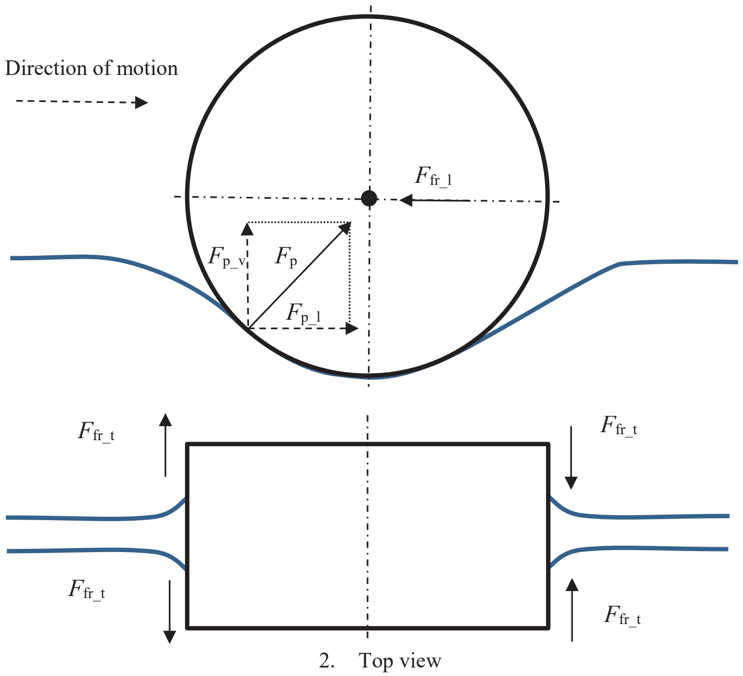

Figure 2: Forces acting in a PLPA experimental setup

Figure 3 presents the experimental setup used to experimentally determine friction effects. The setup includes a PLPA mounted on a carriage and a low friction Airpel Anti-Stiction Air Cylinder, manufactured by Airpot Corp.. The carriage runs over a monorail guidance system manufactured by Rexroth (IMS series). The low friction cylinder can be mechanically connected to the carriage (and hence to the PLPA) to impose external loads. The rollers of the PLPA include ball bearings to reduce friction. The hose tube (with a nominal inner diameter of 25 mm) is composed by a flexible PVC linen reinforced by a high tensile synthetic textile. Its outer layer is covered by light and weather resistant PVC. The hose manufacturer is Dexysflex and the reference used in this work is Tyana SL. On each end of the stroke there are two dampers with a stroke of 40 mm each. The hose length is l=430 mm and the carriage width is 215 mm. The combination of these dimensions allows an available stroke of l_a=180 mm. The setup also includes two servovalves (SV) manufactured by FESTO, model MPYE, that modulate the amount of air flowing into or out each actuator chamber and two proportional pressure (PV) reducing valves, model Sentronic, manufactured by Numatics, to directly control the pressure in each chamber. The servovalves and the pressure reducing valves are connected to the PLPA and the low friction actuator in different ways, described in the next section. All the above described components are connected to a data acquisition and control system comprising a PC with data acquisition boards and all the hardware needed for signal conditioning. The electropneumatic system also includes two pressure transducers, an air treatment unit and a position encoder (5 µm resolution) integrated in the monorail guidance system.

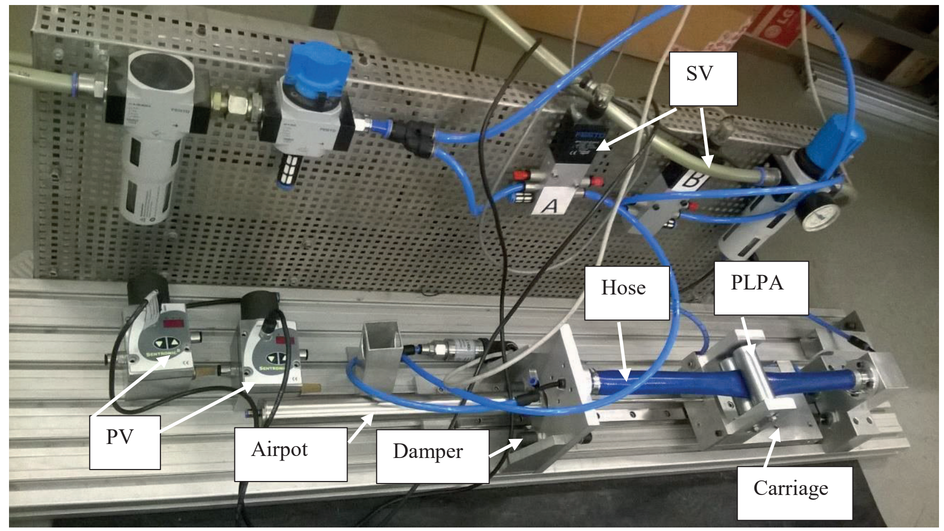

Figure 3: Experimental setup

2.2 Mechanical model

The forces determined in this study are based on the measurement of pressures in the actuator chambers and on the mechanical model. The mechanical model nomenclature is presented in Figure 4.

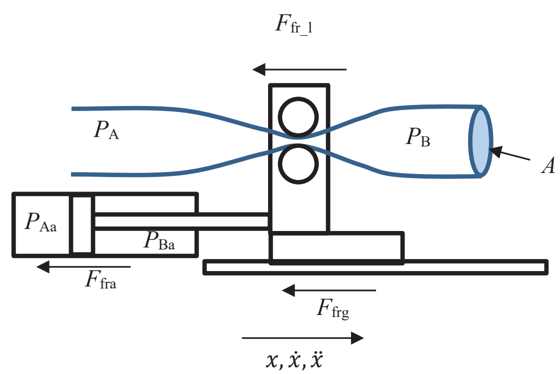

Figure 4: Mechanical model nomenclature

Using Newton's second law, the equilibrium of forces can be written as:

$$M\ddot{x} = F_{p\_l} - F_{fr\_l} + F_{pa} - F_{fra} - F_{frg} \tag{1}$$

where M, $x, \dot{x}, \ddot{x}$ represent the mass, position, velocity and acceleration of the moving mass, respectively. In equation (1), F_{fr_l} represents the friction force acting on the rollers, F_{fra} the friction force acting on the Airpot, F_{frg} the friction force acting on the mechanical guide and F_{p_l}, F_{pa} represent the force exerted by the PLPA and the Airpot actuator, respectively, in the motion direction. Given the deformation of the hose, the area to consider when calculating F_{p_l} is not straightforward. To determine it, a power balance will be performed. Assuming that chamber B of the hose is at atmospheric pressure and that all pneumatic power ($\dot{E}_p$) is converted into mechanical power ($\dot{E}_M$), the following equality can be written for positive direction motion:

$$\dot{E}_p = \dot{E}_m \leftrightarrow P_A Q = F_{p\_l}\dot{x} + F_{p\_t}\dot{x}_t \tag{2}$$

where Q is the volumetric flow rate of air inside the hose A chamber, F_{p_t} is the force exerted by the hose in the transversal direction, and $\dot{x}_t$ is the velocity of the hose in the transversal direction, due to hose flattening. The volumetric flow rate can be written as:

$$Q = A\dot{x} \tag{3}$$

where A represents the hose circular area, since the hose shape far from the rollers is essentially circular as long as pressure is higher than 0.2 bar (cf. next section). Considering the velocity of the hose in the transversal direction to be proportional (by a factor β) to the moving mass linear velocity $\dot{x}$, the mechanical energy spent in the transversal direction can be written as:

$$F_{p\_t}\dot{x}_t = F_{p\_t}\beta\dot{x} \tag{4}$$

Replacing equations (3) and (4) in equation (2) leads to:

$$F_{p\_l} = P_A A - F_{p\_t}\beta \tag{5}$$

Equation (5) shows that part of the available longitudinal force is reduced due to traversal effects. Namely, the force exerted by the hose in the transversal direction must overcome (sliding) friction due to the flattening.

3 Experimental characterization of the PLPA

3.1 Hose shape

The cross sectional area of the PLPA's hose varies not only with pressure but also with the position of the rollers. Regarding the influence of the position of the rollers, the cross section change is due to the flattening of the hose as presented in Figure 5. The region of influence of the hose flattening is axially limited to l_d. In the case of the experimental setup presented in section 2.2, the value of l_d is l_d =65 mm. Notice that large l_d values are undesirable since they reduce the useful stroke of the PLPA.

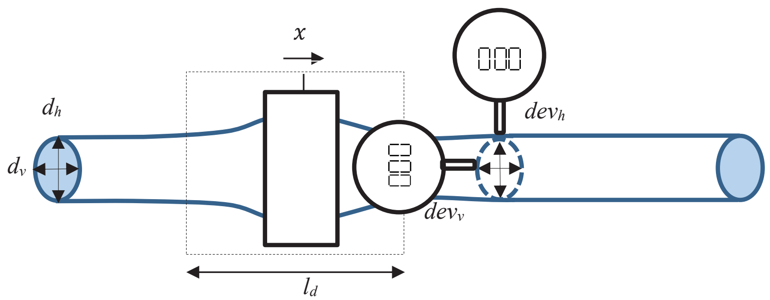

Figure 5: Variation of the hose cross sectional area with the rollers position (top view)

Regarding the influence of pressure in the hose cross section shape, the horizontal (d_h) and vertical (d_v) dimensions were measured for different hose pressures, both in ascending and descending pressure trajectories. Measurements were performed outside the area of influence of the flattening effect. To this end, a digital indicator was used to measure the hose deviations in vertical (dev_v) and horizontal (dev_h) dimensions, as presented in Figure 5. Figure 6 presents the results obtained. Two different behaviours can be observed: whilst in the horizontal direction very small deviations occur, in the vertical dimension deviations are higher. Hysteresis is also more pronounced in the vertical direction. These different behaviours can be explained by the horizontal flattening of the hose caused by the rollers. However, it can be observed that in both cases the deviations for pressures higher than 0.2 bar are limited, in the worst case to ca. 4.8% of the nominal inner diameter of the hose. This means that as long as the inside pressure is higher than 0.2 bar, the hose retains an essentially circular cross section, as can be inferred from Figure 7, where the horizontal and vertical external hose diameters (average values of both trajectories) are presented.

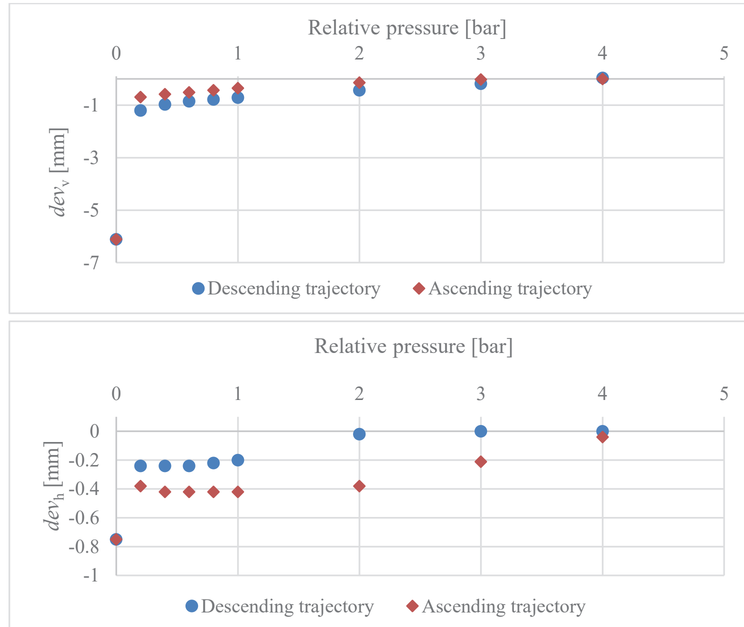

Figure 6: Hose horizontal and vertical deviations with pressure

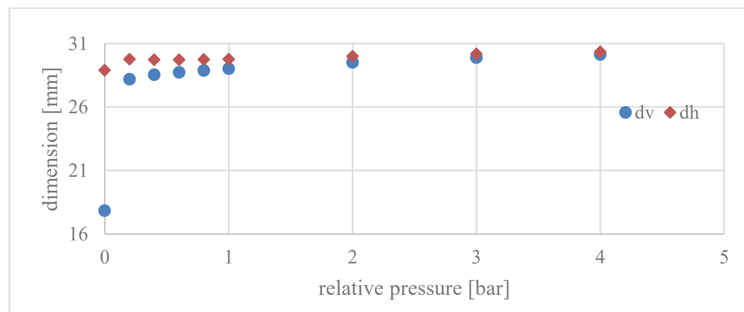

Figure 7: Hose horizontal and vertical external diameters variation with pressure

3.2 Hose static forces

In order to validate the static force capability determined in section 2.3, an experimental assessment was performed. In this experiment, constant pressure levels were imposed on the low friction actuator using pressure reducing valve PR_a and the pressure inside the PLPA was gradually increased using PR_h until motion was detected. In this way, an experimental assessment of the force capability of the PLPA can be determined. Figure 8 shows the experimental setup configuration of this experiment to test the force exerted by the hose left chamber (chamber A). A similar arrangement was made for chamber B.

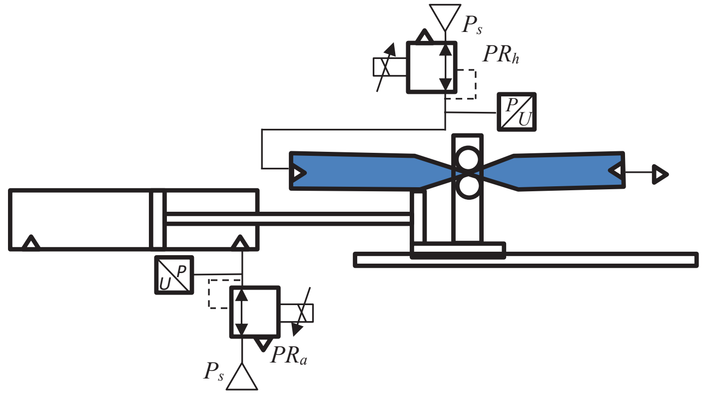

Figure 8: Experimental setup for static force assessment of a PLPA (chamber A)

Results obtained for both chambers are presented in Figure 9 and Figure 10 for chambers A and B, respectively. In these figures, the vertical axis represents the symmetrical pneumatic force exerted by the Airpot cylinder, $-F_{pa}$. In the horizontal axis, the product between hose pressure and area ($P_{A,B} \times A$), is represented. Figures 9 and Figure 10 also indicate the results of a linear regression performed to the respective datasets.

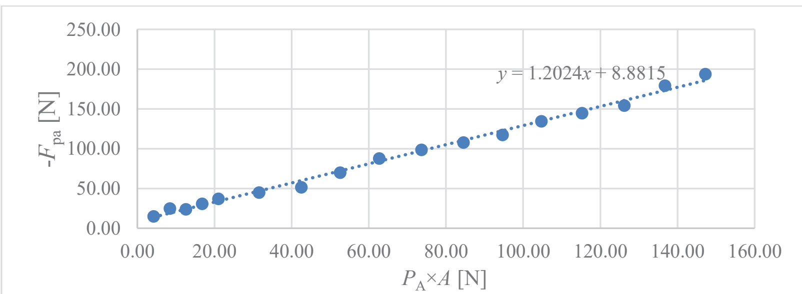

Figure 9: Results obtained in static force assessment of a PLPA (chamber A)

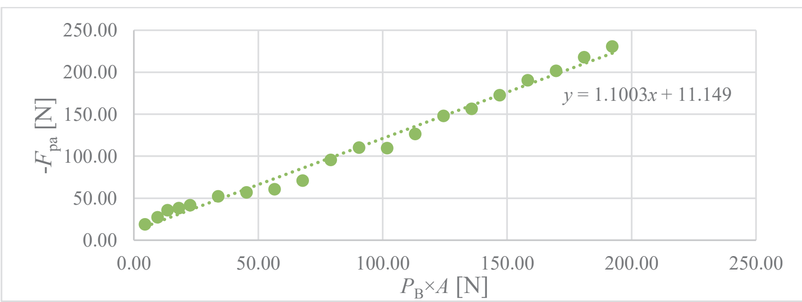

Figure 10: Results obtained in static force assessment of a PLPA (chamber B)

According to equation (1), since these experiments are static, F_{p_l} can be written as:

$$F_{p\_l} = -F_{pa} + F_{fr\_l} + F_{fra} + F_{frg} \tag{6}$$

Replacing equation (5) on equation (6) leads to:

$$P_A A - \left(F_{p\_t}\beta + F_{fr\_l} + F_{fra} + F_{frg}\right) = -F_{pa} \tag{7}$$

The transversal force $F_{p\_t}\beta$ counteracts the transversal friction force due to sliding between hose and rollers when the hose flattens. If there weren't any friction forces present, $P_A \times A = -F_{pa}$ and the linear regression presented in Figure 9 and Figure 10 would have no offset and a gain equal to 1. The sum of the friction components shown in equation (7), F_{frs}, will be modelled as a static (Coulomb) force and by a pressure dependent component, as friction between hose and rollers is likely to increase with pressure. With this assumption, equation (7) can be rewritten as:

$$P_A A - F_{frs} = -F_{pa} \tag{8}$$

where F_{frs} represents all friction forces acting on the system, that can be expressed as:

$$F_{frs} = k_p P_A A + k_0 \tag{9}$$

where k_p is the constant determining the friction pressure dependence and k_0 is the static component. Replacing equation (8) on equation (7) leads to:

$$P_A A\left(1 + k_p\right) + k_0 = -F_{pa} \tag{10}$$

In the present case, using data for both motion directions (cf. Figure 11), k_p =0.1166 and k_0=11.7 N. This means that the static friction force ranges from ca. 5% to ca. 16% of the maximum theoretical force, when pressure varies from 0 to 5 bar, respectively. For comparison purposes, conventional pneumatic rod cylinders present a static friction force ranging from ca. 7% to ca. 10% of the theoretical maximum force /16/. It is therefore possible to state that, when compared to conventional rod actuators, the solution envisaged has lower static friction for low pressures and higher static friction for high pressures. It should be highlighted, nevertheless, that i) no stick slip occurs and ii) rodless actuators (which are comparable to the solution envisaged regarding compactness) present much higher friction values than solutions with rod. It is therefore expectable that the PLPA friction compares favourably with the ones presented by rodless actuators.

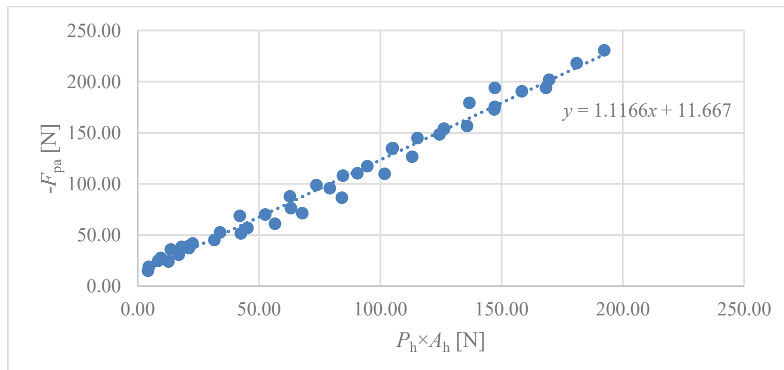

Figure 11: Results obtained in static force assessment of a PLPA

3.3 Velocity control

In order to test the behaviour of the PLPA in conventional velocity control strategies, meter-in and meter-out setups were implemented using the PLPA and the Airpot actuator, as exemplified in Figure 12 for the PLPA and meter-out experiment. A similar setup was performed for meter-in velocity regulation, for both actuators. Three pressure levels (1, 3 and 5 bar, relative) were tested. For each of them three levels of velocity were experimentally tuned, moving in the positive direction. The first level corresponds to “low” velocities and was tuned by changing the valve opening up until motion started. The third level corresponds to “high” velocities obtained by using maximum flow valve openings. The second level corresponds to “medium” velocities, which were tuned to be in between the “low” and “high” levels.

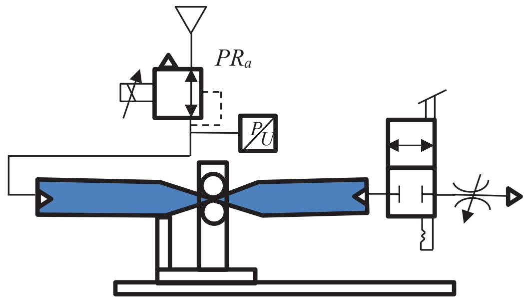

Figure 12: Experimental setup for meter-out velocity control assessment of a PLPA (positive motion)

The results obtained in the PLPA meter-in experiments with P_s= 1 and 5 bar are presented in Figure 13. Figure 14 presents the results obtained in the same conditions but using the Airpot actuator.

Regarding the PLPA, it can be seen that a wide range of velocities is achieved, from ca. 0.05 mm/s, up to 3m/s, obtained for the maximum pressure level, P_s=5 bar. Another interesting feature lies in the absence of stick–slip behaviour in any of the experiments made with the PLPA, contrary to what happens with the Airpot actuator, where this highly undesirable phenomenon occurs (cf. Figure 14 a)). It should be stressed that this behaviour was verified not only under the conditions presented in Figures 13 and 14 (meter-in experiment, P_s= 1 bar and P_s= 5 bar) but also in all other experiment conditions (meter-in experiments with P_s= 3 bar and meter-out experiments with P_s= 1, 3 and 5 bar).

Future studies will consequently focus on using this important feature for servo control purposes. In fact, although irregular motion was sometimes observed in the PLPA, it was detected that those irregularities occurred when the rollers flattened the wrinkles of the hose. This phenomenon was most noticed with low working pressures, when the hose is less stretched.

Another relevant fact lies in the difficulty of tuning different velocities with the PLPA when using P_s=5 bar and meter-out velocity control. In fact, for small and medium restrictor openings, the rollers started to move but then the velocity decreased to very small values. Using high valve openings, the rollers started to accelerate, quickly reaching high velocities. Intermediate velocities were therefore not possible to tune for P_s=5 bar. Contrary to this, the Airpot actuator allowed an easy tuning of intermediate velocities, with the exception meter-in velocity and P_s=1 bar, where the stick-slip phenomenon occurred.

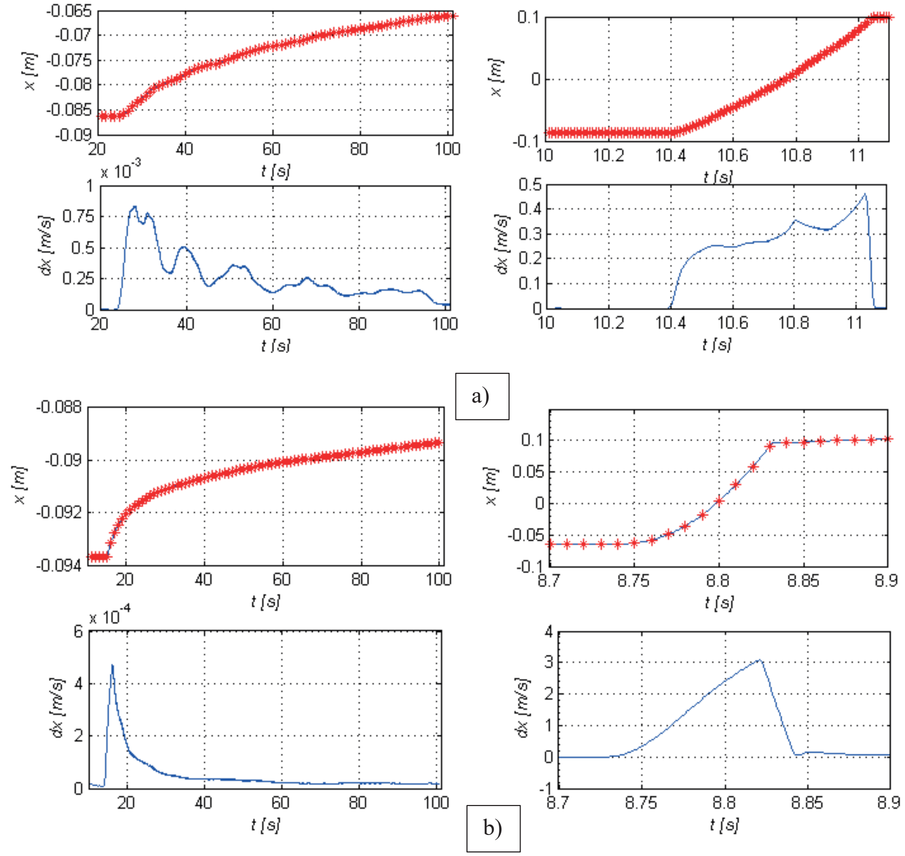

Figure 13: position and velocity results obtained with meter-in velocity control, PLPA, for different source pressure levels and increasing valve openings (left to right): a) P_s = 1 bar, b) P_s = 5 bar

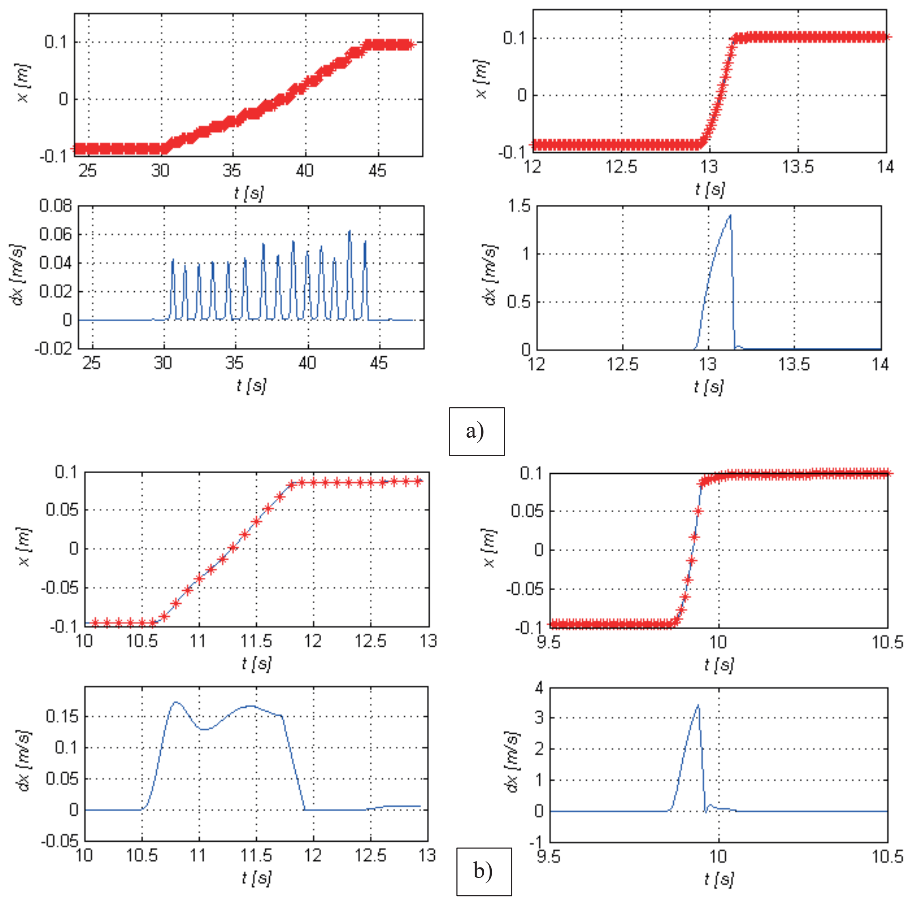

Figure 14: position and velocity results obtained with meter-in velocity control, Airpot, for different source pressure levels and increasing valve openings (left to right): a) P_s = 1 bar, b) P_s = 5 bar

4 Conclusion

This paper presented a peristaltic linear pneumatic actuator for industrial and robotic applications. The solution presented has several potential advantages, namely its low cost, low weight, a virtually unlimited stroke and the ability to perform curved motion profiles. An experimental setup was described and several characteristics were experimentally determined, namely the static force capabilities of proposed actuator. It was shown that the force capabilities of the actuator are similar to those of conventional actuators. Furthermore, it was shown that no stick slip behaviour occurs at low velocities, by experimental trials using conventional meter-in and meter-out control. This important feature will therefore be explored in future studies for servo control. Future topics of research include i) a complete friction characterization of the actuator, ii) the development of alternative mechanical designs so that the effect of the rollers inter-axial spacing can be studied iii) a hose endurance analysis and iv) the analysis of the system behaviour using curved mechanical guides.

5 Acknowledgements

The authors gratefully acknowledge the funding of Project NORTE-01-0145-FEDER-000022 - SciTech - Science and Technology for Competitive and Sustainable Industries, cofinanced by Programa Operacional Regional do Norte (NORTE2020), through Fundo Europeu de Desenvolvimento Regional (FEDER).

References

/1/ Merkelbach, S., H. Murrenhoff, B. C., M. Fey, and B. Eßer. Pneumatic or electromechanical drives – a comparison regarding their exergy efficiency. in 10th International Fluid Power Conference. 2016. Dresden, Germany.

/2/ Gauchel, W. and S. Haag. Servopneumatic Clamping System for the Assembly of Battery Cells in the Area of Electromobility in 10th International Fluid Power Conference 2016. Dresden, Germany.

/3/ Rakova, E., J. Hepke, and J. Weber. EXonomy analysis for the Inter-domain comparison of electromechanical and pneumatic drives. in 10th International Fluid Power Conference 2016. Dresden, Germany.

/4/ Carneiro, J.F. and F.G. Almeida, Micro tracking and positioning using off-the-shelf servopneumatics. Robotics and Computer Integrated Manufacturing, 2014. 30(3): p. 244-255.

/5/ Falcão Carneiro, J. and F. Gomes de Almeida, Accurate motion control of a servopneumatic system using integral sliding mode control. Int. J. of Adv. Manuf. Technol., 2014. 77(9): p. 1533-1548.

/6/ Carneiro, J.F. and F.G. Almeida, A high accuracy trajectory following controller for pneumatic devices. Int. J. of Adv. Manuf. Technol., 2012. 61(1): p. 253-267.

/7/ Carneiro, J.F. and F.G. Almeida, A macro-micro motion servopneumatic device. Proc. of the Inst. of Mech. Eng., Part I: J. of Syst. and Control Eng., 2012. 226(6): p. 775-786.

/8/ Weist, J., M. Arteaga, L. de la Cruz, and H. Hebisch, Model free control for differential pneumatic pistons: experimental comparison. International Journal of Control, 2011. 84(1): p. 138-164.

/9/ Girin, A., F. Plestan, X. Brun, and A. Glumineau, High-Order Sliding-Mode Controllers of an Electropneumatic Actuator: Application to an Aeronautic Benchmark. IEEE Trans. Control Syst. Technol., 2009. 17(3).

/10/ Suzumori, K., A. Wada, and S. Wakimoto, New mobile pressure control system for pneumatic actuators, using reversible chemical reactions of water. Sensors and Actuators A: Physical, 2013. 201: p. 148-153.

/11/ Wada, A., H. Nabae, T. Kitamori, and K. Suzumori, Energy regenerative hose-free pneumatic actuator. Sensors and Actuators A: Physical, 2016. 249: p. 1-7.

/12/ Li, H., K. Kawashima, K. Tadano, S. Ganguly, and S. Nakano, Achieving Haptic Perception in Forceps' Manipulator Using Pneumatic Artificial Muscle. IEEE/ASME Trans. on Mechatron., 2013. 18(1): p. 74-85.

/13/ Bone, G., M. Xue, and J. Flett, Position control of hybrid pneumatic–electric actuators using discrete-valued model-predictive control. Mechatronics, 2015. 25: p. 1-10.

/14/ Ashby, G. and G. Bone. Improved Hybrid Pneumatic-Electric Actuator for Robot Arms. in 2016 IEEE International Conference on Advanced Intelligent Mechatronics (AIM). 2016. Banff, Alberta, Canada, .

/15/ Goldin, R., Pneumatischer oder hydraulischer Linearantrieb, 1984: Germany. p. 18.

/16/ Falcão Carneiro, J. and F. Gomes Almeida. LuGre friction model: application to a pneumatic actuated system. in Controlo 2014, 11th Conference on Automatic Control. 2014. Porto, Portugal.